



Figure SI 1. Evolution of the colour of the $\text{SmCr}_{1-x}\text{Fe}_x\text{TiO}_5$ powders from $x = 0$ (left) to 1 (right).

Table SI 1. RT crystallographic parameters of $\text{SmCr}_{1-x}\text{Fe}_x\text{TiO}_5$ samples with $x = 0.25, 0.5, 0.75$ and 1 , from SXRPD data. Parameters of SmCrTiO_5 ($x = 0$) are reported elsewhere¹. Cell parameters and compositions of the $4f$ and $4h$ sites (versus x) are given in Table 1.

Element	Wyckoff site	x (Fe content)	x	y	z	B (\AA^2)
Sm	$4g$	0.25	0.13915(6)	0.17124(7)	0	0.494(8)
		0.5	0.13822(8)	0.17086(8)		0.60(1)
		0.75	0.13715(8)	0.17060(8)		0.464(9)
		1	0.13636(7)	0.17048(7)		0.62(1)
$M1_{\text{oct}}$	$4f$	0.25	0	1/2	0.2479(3)	0.17(3)
		0.5			0.2483(3)	0.23(3)
		0.75			0.2481(3)	0.44(3)
		1			0.2486(3)	0.50(3)
$M2_{\text{pyr}}$	$4h$	0.25	0.1169(2)	-0.1447(2)	1/2	0.19(3)
		0.5	0.1160(2)	-0.1448(2)		0.19(4)
		0.75	0.1148(2)	-0.1447(2)		0.43(3)
		1	0.1137(2)	-0.1444(2)		0.44(3)
O1	$8i$	0.25	0.1051(5)	-0.2902(4)	0.2546(6)	0.87(9)
		0.5	0.1064(6)	-0.2905(5)	0.2538(6)	1.0(1)
		0.75	0.1058(6)	-0.2908(5)	0.2516(6)	0.6(1)
		1	0.1063(5)	-0.2914(5)	0.2518(6)	0.8(1)
O2	$4g$	0.25	0.1612(8)	0.4451(7)	0	1.2(1)
		0.5	0.1617(9)	0.4469(7)		1.2(1)
		0.75	0.1637(9)	0.4454(7)		1.0(1)
		1	0.1637(8)	0.4456(7)		1.0(1)
O3	$4h$	0.25	0.1600(8)	0.4258(6)	1/2	0.8(1)
		0.5	0.1579(9)	0.4264(7)		1.0(1)
		0.75	0.1577(10)	0.4258(7)		1.0(1)
		1	0.1584(9)	0.4249(7)		1.1(1)
O4	$4e$	0.25	0	0	0.2851(9)	0.5(1)
		0.5			0.2857(9)	0.8(1)
		0.75			0.2815(10)	0.3(1)
		1			0.2803(9)	0.2(1)

¹ A. E. Susloparova, J. P. Bolletta, B. Kobzi, A. A. Paecklar, S. Jouen, F. Fauth, V. Nachbaur, V. Nassif, E. Suard, D. Sedmidubsky, A. I. Kurbakov, A. Maignan, and C. Martin, Structural and magnetic properties of SmCrTiO_5 , *Phys. Rev. B*, 2024, **110**, 224429, DOI: 10.1103/PhysRevB.00.004400

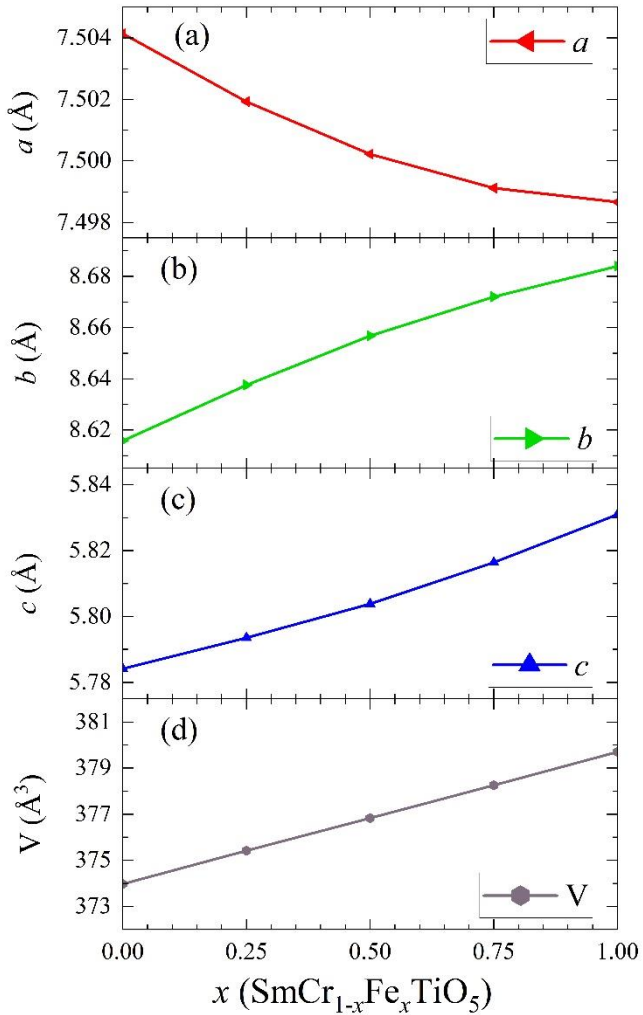


Figure SI 2. Unit cell parameters (a-c) and volume (d) vs x for $\text{SmCr}_{1-x}\text{Fe}_x\text{TiO}_5$.
Error bars are smaller than symbol size in all cases.

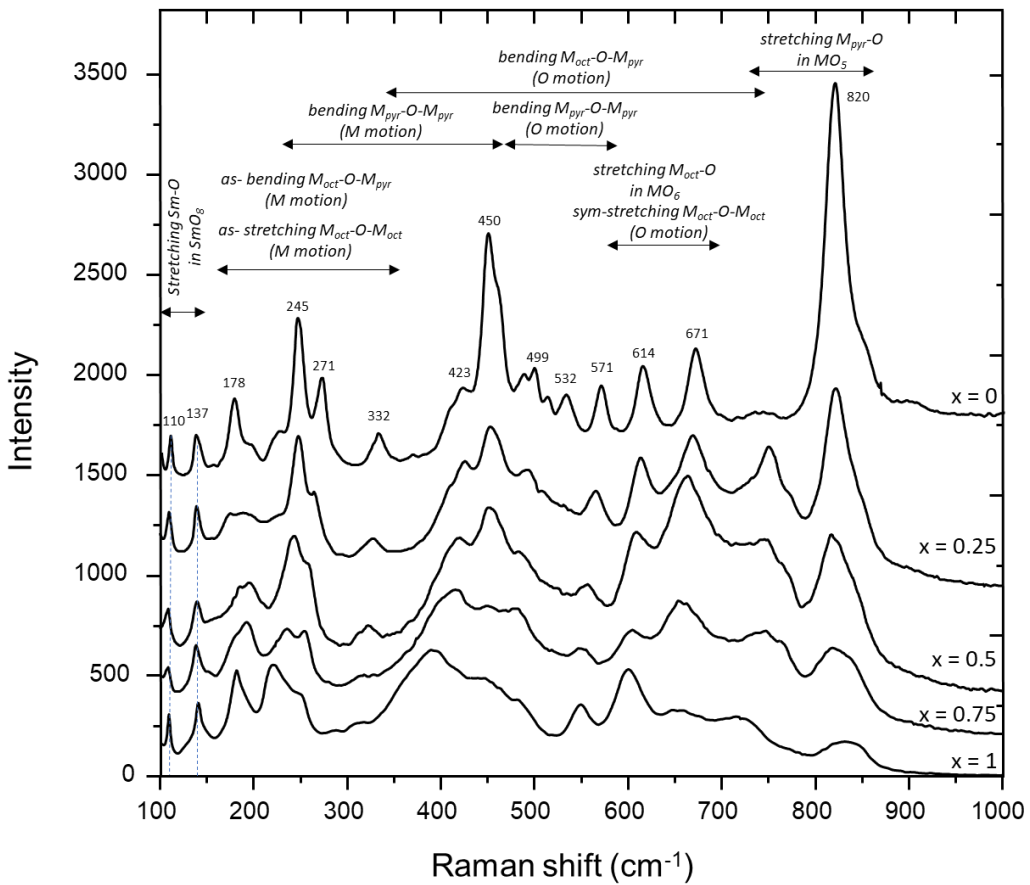


Figure SI 3. RT Raman spectra of $\text{SmCr}_{1-x}\text{Fe}_x\text{TiO}_5$ with $x = 0, 0.25, 0.5, 0.75$, and 1 .

Arrows indicate the frequency range assigned to the different vibrational units.

(*as-* = asymmetric mode; *sym-* = symmetric mode)

The assignment of the peaks is based on the shell model calculation performed by Litvinchuk's on the isostructural compound RMn_2O_5 ($R = \text{Ho, Dy}$)¹ and the analyses reported for NdCrTiO_5 ², GdCrTiO_5 ³, NdMnTiO_5 ⁴ and BiMn_2O_5 ⁵. The assignment of each Raman peak to specific vibrational units is error-prone because of the overlapping between the absorption range of the multiple vibrational units of the structure, so only the modification in the spectra with iron content is described hereafter in three different frequencies ranges.

- The lowest frequency region $< 150 \text{ cm}^{-1}$ is attributed to vibrations involving the heaviest atoms, i.e., internal Sm-O stretching vibrations in the SmO_8 units. The position of the peaks (110 cm^{-1} and 137 cm^{-1}) does not change with x which indicates that the SmO_8 polyhedron is not modified by the iron for chromium substitution.

- The medium frequency range [$150 - 750 \text{ cm}^{-1}$] is assigned to several bending and stretching vibrational modes of the $M_{\text{oct}} - \text{O} - M_{\text{oct}}$, $M_{\text{pyr}} - \text{O} - M_{\text{oct}}$, $M_{\text{pyr}} - \text{O} - M_{\text{pyr}}$ structural units ($M_{\text{oct}} = \text{Cr}^{3+}$, Ti^{4+} or Fe^{3+} and $M_{\text{pyr}} = \text{Ti}^{4+}$ or Fe^{3+}), caused by M and O motions in the lowest and highest energy range, respectively and also by stretching vibration in the MO_6 units. The peaks are broader and shifted towards the lower frequencies with

increasing iron content. The broadening is explained by the mixing of individual contributions related to additional vibrational units, reflecting thus the mixed occupation of the sites and the shifts are correlated to higher amount of iron in the two sites when x increases, as shown from Mossbauer study (Table 2).

- Beyond 750cm^{-1} , the vibrational modes are assigned to the symmetrical stretching $M\text{-O}$ vibrations in the pyramidal site. For $x = 0$, the very intense peak located at 820 cm^{-1} is attributed to internal vibrations in TiO_5 polyhedra^{3,6}. As the iron content increases, the relative intensity of this peak decreases drastically, suggesting the presence of iron into the square-pyramidal site with titanium. The appearance of a new peak at lower frequencies, around 750 cm^{-1} , supports this hypothesis of the substitution of Ti^{4+} by Fe^{3+} in the square pyramid as it probably corresponds to internal Fe - O stretching vibrations in FeO_5 units.

¹ A. P. Litvinchuck, Lattice dynamics and spin–phonon interactions in multiferroic RMn_2O_5 : Shell model calculations, Journal of Magnetism and Magnetic Materials 321 (2009) 2373–2377 DOI: 10.1016/j.jmmm.2009.02.122

² K. Gautam, A. Ahad, K. Dey, S. S. Majid, S. Francoual, V. G. Sathe, Ivan da Silva, and D. K. Shukla, Symmetry breaking and spin lattice coupling in NdCrTiO_5 , Phys. Rev. B 100, 104106 (2019) DOI: 10.1103/PhysRevB.100.104106

³ T. Basu, K. Singh, S. Gohil, S. Ghosh, and E. V. Sampathkumaran, Implications of magnetic and magnetodielectric behavior of GdCrTiO_5 , J. Appl. Phys.118, 234103 (2015) DOI:10.1063/1.4937399

⁴ K. Ghosh, M. M. Murshed, T. Frederichs, N.K.C. Muniraju, T. M. Gesing, Structural, vibrational, thermal, and magnetic properties of mullite-type NdMnTiO_5 , J Am Ceram Soc.105:2702–2712 (2022) DOI: 10.1111/jace.18261

⁵ F.M. Silva Júnior, C.W.A. Paschoal, R.M. Almeida, R.L. Moreira, W. Paraguassu, M.C. Castro Junior, A.P. Ayala, Z.R. Kann, M.W. Lufaso, Room-temperature vibrational properties of the BiMn_2O_5 mullite, Vibrational Spectroscopy 66 (2013) 43– 49 DOI: dx.doi.org/10.1016/j.vibspec.2013.01.010

⁶ M. Th. Paques-Ledent, Infrared and Raman studies of M_2TiO_5 compounds (M = rare earths and Y): isotopic effect and group theoretical analysis, Spectrochimica Acta, Vol. 32A, pp 1339 - 1344 DOI: 10.1016/0584-8539(76)80177-8

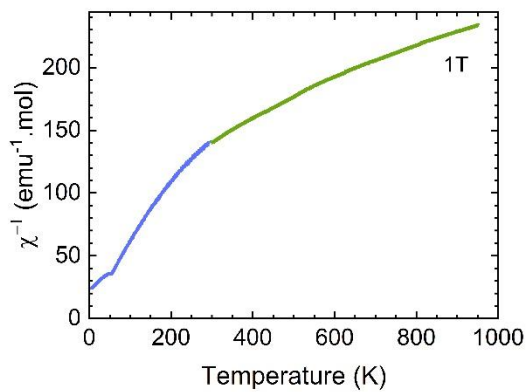


Figure SI 4. Inverse of the magnetic susceptibility curves of SmFeTiO_5 versus temperature.

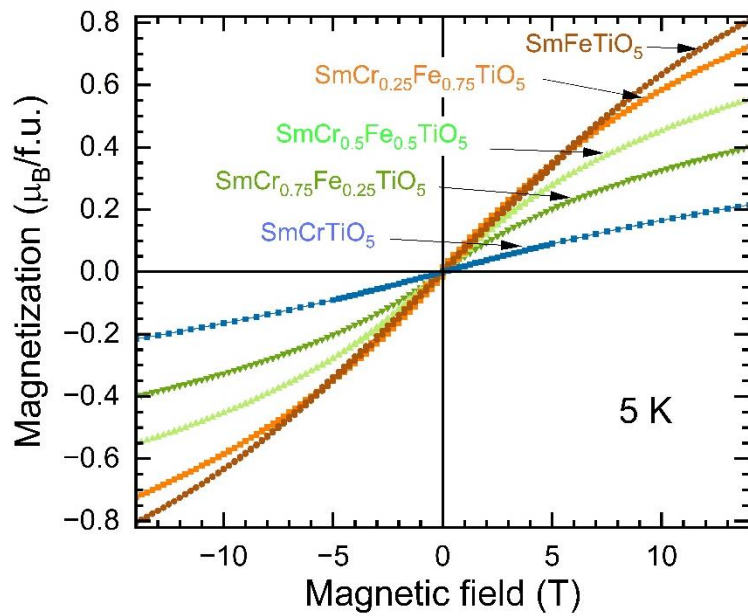


Figure SI 5. Magnetization vs magnetic field ($0 \rightarrow +14 \text{ T} \rightarrow -14 \text{ T} \rightarrow +14 \text{ T}$) curves recorded at 5 K of the five $\text{SmCr}_{1-x}\text{Fe}_x\text{TiO}_5$ samples ($x = 0, 0.25, 0.5, 0.75$ and 1).